PHYSICAL REVIEW C VOLUME 23, NUMBER 2 FEBRUARY 1981

# $^3$He and $^3$H bound state for the Reid soft-core potential

T. Sasakawa and H. Okuno
*Department of Physics, Tohoku University, 980 Sendai, Japan*

T. Sawada
*Department of Applied Mathematics, Faculty of Engineering Science, Osaka University, 560 Toyonaka, Japan*
(Received 28 May 1980)

The perturbational approach that has been used for the calculation of the triton bound state is applied to $^3$He. The Coulomb potential is fully taken into account within the limitation of the Reid soft-core-3 potential. We obtain 5.775 MeV as the binding energy of $^3$He. The Coulomb energy difference with $^3$H is 0.625 MeV. The Coulomb effects to the charge form factor and the two-body correlation function are calculated. Qualitative discussions are given for the complex behavior of the Faddeev components expressed in terms of the spectator momentum and the relative distance of the interacting pair.

[NUCLEAR STRUCTURE $^3$He and $^3$H bound state. Exact solution of the Faddeev equation by a perturbative approach. Binding energy of $^3$He: 5.775 MeV. Coulomb energy difference with triton: 0.625 MeV. Coulomb effects to charge form factor and correlation function.]

## I. INTRODUCTION

For a long time, the Faddeev equation for $^3$H has attracted a great deal of attempts to solve it. A number of methods have been proposed and proved to be successful. At present, all calculations for the Reid soft-core (RSC) potential[1] (RSC; $^1S_0$, $^3S_1$-$^3D_1$) have reached an agreement as to the binding energy of $^3$H: about 6.4 MeV with the spectator $s$ state [Reid soft-core-3 potential (RSC3)] (Refs. 2–6) and about 7.0 MeV with the additional spectator $d$ state for the interacting $^3S_1$-$^3D_1$ states [Reid soft-core-5 potential (RSC5)].[7-9]

On the other hand, we feel a necessity to explore a technique for solving the Faddeev equation for $^3$He that includes the Coulomb interaction as well as a realistic nuclear interaction. In fact, only one method, that is to solve the partial differential equation with hyperspherical coordinates, was so far successful.[10,11] However, the Coulomb energy difference obtained directly from the solution of this method is much smaller than the value expected from the usual perturbational calculations, because all partial waves of the Coulomb potential are not retained. The eigenvalue difference for the $s$-wave projected Coulomb potential problem of Ref. 11 was 546 keV,[12] whereas including the higher partial waves, the first order perturbation yielded 0.61 MeV.[10,11,13] Malfliet and Tjon[14] obtained 0.63 MeV by the perturbation theory for the Reid soft-core-4 potential (RSC4) (the spectator $d$ state for the interacting $^3S_1$ state in addition to RSC3). We also remark that in all articles, except Ref. 10, the charge form factor for $^3$He has been calculated with the wave function of $^3$H. With this background, we present a new technique for handling $^3$He.

In many cases, the Faddeev equation (for $^3$H) has been solved by means of various separable expansions of the two-body $t$ matrix. However, the $t$ matrix for a local potential cannot exactly be expressed as a sum of separable terms.[15] Also, a complete orthonormal set of functions, such as the Sturm-Liouville function, the harmonic oscillator function, or the $K$-harmonic function, has sometimes been utilized to expand the two-body $t$ matrix or the three-body wave function.[4] However, the convergence becomes very slow in many cases, and also the increasing number of nodes prevents us from performing accurate numerical calculations. For these reasons, one is forced to truncate the expansion, with the result that the short range behavior is not accurately reproduced.

These difficulties are avoided in the new perturbational approach introduced in our previous paper.[4] The basic idea was to extract terms that might cause divergence or converge very slowly, express these terms as separable, and treat them as the zeroth order term in iterations, all of the remainder being treated as the perturbation. To be more specific, the contributions from the first Sturm-Liouville eigenstates are chosen as the unperturbed term. By this method, a quick convergence is almost evident *ab initio*, and it has been demonstrated to be the case.[4] It should be noted that in this perturbation method, we need not introduce a truncation of the kind that is needed in the method of expansion by a complete set.

 

We have treated the two-body interaction in coordinate space. By doing this, we avoid the difficulty of truncation at large momentum that is effective near the origin of the Reid soft-core potential.

Let us discuss some aspects concerning the accuracy of Ref. 4. In Refs. 3 and 8, for example, ten and sixteen mesh points are chosen for the spectator and the relative motion in momentum space, respectively. We should handle an $800\times 2$ matrix for each step. In Ref. 4, to be accurate everywhere, we have used 30 uneven mesh points for the distance $x$ of the interacting pair from $x=0$ to 6 fm with the mesh size ranging from $x=0.0270$ fm at $x=0$ fm to 0.725 fm at $x=6$ fm, and an analytic formula beyond 6 fm. Our smallest mesh point corresponds to the cutoff momentum of about 40 $\text{fm}^{-1}$. This should be compared with the cutoff momentum of 13 $\text{fm}^{-1}$ in Refs. 3 and 8. For the spectator, we have used the momentum space representation with twelve mesh points. Therefore, the number of mesh points as well as the cutoff momentum in Ref. 4 are much larger than those in Refs. 3 and 8. The theory is formulated so that the dimensionality of the matrix from which the binding energy is obtained is as small as possible. Thus the dimensionality is only 12 in Ref. 4. The binding energy is very accurately determined from this matrix as seen from Fig. 5 of Ref. 4.

The Coulomb potential was not involved in Ref. 4. The Faddeev equation describes a sequence of multiple scatterings, in which a third particle moves freely as a spectator while the other two particles are interacting.[16] However, since the Coulomb potential is a long range potential, the "spectator" which is free from the short range interaction must be under the influence of the Coulomb potential. A method of accommodating the Coulomb potential according to this physical picture was given in another paper[17] which the present paper follows closely. A technical difficulty of expressing the Coulomb wave function described in one set of the Jacobi coordinates by another set has been numerically overcome owing to the short range nature of the interacting kernel of Ref. 17.

For the Coulomb wave functions, we have used the very accurate Saclay-code CEA-N-906. For the two-body correlation, we have maintained a similar accuracy as in Ref. 4. We have employed the spline interpolation in expressing the Coulomb wave function described in one set of coordinates by another. For testing the accuracy of the present calculation, we have switched off the Coulomb potential in the code PERFECT III that was made for the present purpose and compared the results with those calculated by the code PERFECT I[18] used in Ref. 4. Despite the complete difference in the numerical treatment of very involved parts of expressing the function described in one set of coordinates by another, we have obtained a remarkable agreement of numerical results.

It is known that by the method of Ref. 7, the treatment of very low energy $n$-$d$ or $p$-$d$ scatterings is difficult in practice. On the other hand, our method has no practical difficulty, since we can make use of analytic expressions around the peripheral region or in the wave zone.

In the present paper, we focus our attention on the formulation and the study of the nature of the solution of the generalized Faddeev equation with Coulomb interaction and some direct consequences. The comparison of the charge form factor of $^3$He with and without Coulomb effect in the wave function is made. To our knowledge, this is the first exact presentation of the Coulomb effect on the charge form factor. Also we obtained the Coulomb energy difference which is almost equal to that from the perturbational calculations. Some results of physical interest will appear in separate articles.[19,20]

In Sec. II, the generalized Faddeev equation involving the Coulomb effect is expressed in the form of an integral equation. In Sec. III, the outline of the formulation and the iterative procedure are demonstrated. In Sec. IV, the numerical method and results are presented. In Sec. V, discussions and conclusions are given.

## II. GENERALIZED FADDEEV EQUATION

For the most part, the notations and basic concepts are the same as in Ref. 4. However, we repeat some of them to the extent that the present paper is self-contained.

We use the set of coordinates and momenta

$$\vec{x}_3=\vec{r}_1-\vec{r}_2,\quad \vec{y}_3=\vec{r}_3-(\vec{r}_1+\vec{r}_2)/2\,, \tag{1}$$

and

$$\vec{p}_3=\tfrac{2}{3}[\vec{k}_3-(\vec{k}_1+\vec{k}_2)/2]\,. \tag{2}$$

We suppress the suffixes of $\vec{x}$, $\vec{y}$, and $\vec{p}$ whenever there is no possibility of confusion. Since we are treating the problem in coordinate space, to each momentum $p$ of the spectator particle there corresponds a momentum $q$ of the interacting pair through the relation

$$|q|=(m|E|/\hbar^2+3p^2/4)^{1/2}\quad (q=i|q|)\,, \tag{3}$$

where $|E|$ denotes the binding energy of the three nucleon system. Henceforth, we use the notation $q$ in place of $|q|$ for simplicity.

If the function $\Phi(12,3)$ is antisymmetric with respect to the exchange of 1 and 2, the totally antisymmetric three-body wave function is given by

$$\Psi = \Phi(12,3) + \Phi(23,1) + \Phi(31,2). \quad (4)$$

The component $\Phi(12,3)$ satisfies the generalized Faddeev equation[17]

$$(E - H_0 - V_{12} - u^c_{12} - u^c_{3,1} - u^c_{3,2})\Phi(12,3) = (V_{12} + u^c_{12} - u^c_{1,2})\Phi(23,1) + (V_{12} + u^c_{12} - u^c_{2,1})\Phi(31,2). \quad (5)$$

Other Faddeev components satisfy the equations which are obtained from Eq. (5) by cyclic permutations of 1, 2, and 3.

In Eq. (5), $u^c_{12}$ denotes the Coulomb interaction acting on the pair 12,

$$u^c_{12} = v^c(x_3)\frac{1+\tau_{1z}}{2}\frac{1+\tau_{2z}}{2}, \quad (6)$$

where $v^c(x)$ is the Coulomb potential

$$v^c(x) = \frac{e^2}{x}. \quad (7)$$

Here, $\tau_{iz}$ is the third component of the isospin operator of the particle $i$. The potential $u^c_{i,j}$ is a regularized Coulomb interaction which is a function of $y_i$, and defined so that it becomes $e^2/y_i$ in the limit of $y_i \to \infty$. More specifically, it is defined by

$$u^c_{i,j}(y_i) = \bar{v}^c(y_i)\frac{1+\tau_{iz}}{2}\frac{1+\tau_{jz}}{2}. \quad (8)$$

The potential $\bar{v}^c(y_i)$ is chosen so that

$$\bar{v}^c(y_i) \xrightarrow[y_i\to\infty]{} \frac{e^2}{y_i}, \quad \xrightarrow[y_i\to 0]{} \text{constant}. \quad (9)$$

In the present paper, we adopt the following form

$$\bar{v}^c(y) = (1 - e^{-\lambda y})\frac{e^2}{y}. \quad (10)$$

We have introduced the interaction (8) in Eq. (5) for two reasons. Firstly, when the spectator and one of the interacting particles are charged, the spectator is subject to the Coulomb potential. Secondly, in the limit of $x_3 \to \infty$ or $y_1 \to \infty$, the Coulomb effect $u^c_{12} - u^c_{1,2}$ becomes as small as $O(x_3^{-2})$. This property helps the numerical calculation.

We use the isospin function $|II_z, \frac{1}{2}m_t; M_T)$, where $I$, $I_z$, $m_t$, and $M_T$ denote the isospin of the interacting pair, the third component of it, the third component of the isospin $t(=\frac{1}{2})$ of the spectator, and that of the total isospin $T$, respectively. For $^3$He, $T$ takes the values of either $\frac{1}{2}$ or $\frac{3}{2}$. The isospin functions for $^3$He are shown in Table I.

We introduce a set of functions

$$|\vec{F}_{\underline{\alpha}}) = |\vec{\alpha})F_\alpha(p,y). \quad (11)$$

Here $|\vec{\alpha})$ denotes the spin-isospin-angular function. The arrow indicates that, in the case of $^3S_1$ and $^3D_1$ states, the spin-angular function is represented by a $1\times 2$ matrix. The function $|\alpha)$ is one component of $|\vec{\alpha})$,

$$|\alpha) = |(LS)J; (l\tfrac{1}{2})j; J_0 M_0)|II_z; \tfrac{1}{2}m_t; M_T). \quad (12)$$

The capital (small) letters $(LS)J[(l\frac{1}{2})j]$ stand for the interacting pair (spectator). $J_0$ and $M_0$ represent the total angular momentum and its $z$ component of the system, respectively. The underline under $\alpha$ of $|\vec{F}_{\underline{\alpha}})$ implies the $p$ dependence of $F_\alpha(p,y)$.

The function $F_\alpha(p,y)$ represents the radial function of the spectator. It is given by

$$F_\alpha(p,y) = \begin{cases} (2/\pi)^{1/2} p j_l(py), & \text{for state No. 2 of Table I,} \\ F^c_\alpha(p,y), & \text{for states No. 1 and No. 3 of Table I.} \end{cases} \quad (13)$$

The function $F^c_\alpha(p,y)$ stands for a regular solution of the Schrödinger equation for the spectator with the modified Coulomb interaction $\bar{v}^c(y)$. The function $F_\alpha(p,y)$ is orthonormalized so that

$$(\alpha, F_\alpha(p,y)|\alpha', F_{\alpha'}(p',y)) = \delta_{\alpha\alpha'}\delta(p-p'). \quad (14)$$

Here, ( | and | ) are taken for the same partition, e.g., for (12,3). The inner product ( | ) represents the sum and integration over all coordinates except $x = |\vec{x}|$.

We expand the function $|\Phi(12,3)\rangle$ in terms of $|\vec{F}_{\underline{\alpha}})$ as follows.

$$\Phi(12,3) = S_{\vec{\underline{\alpha}}}|\vec{F}_{\underline{\alpha}}(12,3))(\vec{F}_{\underline{\alpha}}(12,3)|\Phi(12,3)\rangle. \quad (15)$$

Here $S_{\vec{\underline{\alpha}}}$ denotes the integration over $p$ and the sum over $\vec{\alpha}$.

Multiplying Eq. (5) by the function $(\vec{F}_{\underline{\alpha}}(12,3)|$, we obtain

$$\left[-\frac{q^2}{M} - \vec{T}_L(x) - \vec{V}_a(x) - \vec{u}^c_a(x)\right](\vec{F}_{\underline{\alpha}}|\Phi\rangle = (\vec{F}_{\underline{\alpha}}|VP|\Phi\rangle + (\vec{F}_{\underline{\alpha}}|\Delta u^c|\Phi\rangle, \quad (16)$$

where $\vec{T}_L(x)$ denotes the kinetic energy operator for the relative motion of the interacting pair with angular momentum $L$, and $\vec{V}_a(x)$ and $\vec{u}^c_a(x)$ are defined, respectively, by

$$\vec{V}_a(x) \equiv (\vec{a}|V|\vec{a}) \text{ and } \vec{u}^c_a(x) \equiv (\vec{a}|u^c|\vec{a}). \quad (17)$$

The function $|\vec{a})$ stands for the two-body spin-isospin-angular function involved in $|\vec{a})$. The matrix $(\vec{a}|V|\vec{a})$ is a $2\times 2$ matrix for the $^3S_1$-$^3D_1$ coupled

TABLE I. Isospin functions for the first component. $I$ and $I_z$ ($t$ and $m_t$) denote the isospin and its third component of the interacting pair (spectator). $M_T$ stands for the third component of the total isospin. Isospin functions for other components are obtained by the cyclic permutations of 1, 2, and 3.

| State | $I$ | $I_z$ | Pair | $\vert II_z;tm_t;M_T(12,3))$ |
|---|---|---|---|---|
| No. 1 | 1 | 0 | $np$ | $\vert 10;\frac{1}{2}\frac{1}{2};\frac{1}{2}(12,3)) = -\frac{1}{\sqrt{2}}\vert(p_1n_2+n_1p_2)p_3)$ |
| No. 2 | 1 | 1 | $pp$ | $\vert 11;\frac{1}{2}-\frac{1}{2};\frac{1}{2}(12,3)) = p_1p_2n_3$ |
| No. 3 | 0 | 0 | $np$ | $\vert 00;\frac{1}{2}\frac{1}{2};\frac{1}{2}(12,3)) = \frac{1}{\sqrt{2}}\vert(p_1n_2-n_1p_2)p_3)$ |

states. The notation $P$ represents the permutation operator,

$$P\Phi = P\Phi(12,3) = \Phi(23,1)+\Phi(31,2). \tag{18}$$

The potential $\Delta u^c$ is defined by

$$\Delta u^c\vert\Phi\rangle = (u^c_{12}-u^c_{1,2})\vert\Phi(23,1)\rangle + (u^c_{12}-u^c_{2,1})\vert\Phi(31,2)\rangle. \tag{19}$$

A more explicit presentation of Eq. (16) in terms of the antisymmetric wave function of $^3$He was given in another paper.[21] However, in the present paper, we do not write out Eq. (16) in more detail, because the more explicit expression is clear if we refer to Ref. 21.

Let us express Eq. (16) in the form of an integral equation. For this purpose, we define the two-body Green's function by

$$\vec{G}^{c(2)}_{\underline{a}} \equiv \frac{1}{-\hbar^2q^2/M-\vec{T}_L-\vec{V}_a-\vec{u}^c_a} = \vec{G}^{c(2)}_{\underline{a},0}+\vec{G}^{c(2)}_{\underline{a},0}\vec{V}_a\vec{G}^{c(2)}_{\underline{a}}. \tag{20}$$

Of course, for state Nos. 1 and 3 of Table I, we should drop the Coulomb potential $\vec{u}^c_a$, as well as all superscript $c$'s, meaning "Coulomb." However, throughout the present paper, we keep the notation $c$ to remind that the Coulomb effect is involved in the theory. In Eq. (20), the superscript (2) represents that the Green's function is defined in the two-body space.

For a bound state, the function $(\vec{F}_{\underline{a}}\vert\Phi\rangle$ of Eq. (16) is represented in terms of the two-body $t$ matrix defined by

$$\vec{G}^{c(2)}_{\underline{a}}\vec{V}_a = \vec{G}^{c(2)}_{\underline{a},0}\vec{t}_a, \tag{21}$$

as the solution of the homogeneous integral equation

$$(\vec{F}_{\underline{a}}\vert\Phi\rangle = \vec{G}^{c(2)}_{\underline{a},0}\vec{t}_{\underline{a}}(\vec{F}_{\underline{a}}\vert P\vert\Phi\rangle+\vec{G}^{c(2)}_{\underline{a}}(\vec{F}_{\underline{a}}\vert\Delta u^c\vert\Phi\rangle. \tag{22}$$

Accordingly, the function $\vert\Phi\rangle[=\Phi(12,3)]$ is represented as

$$\vert\Phi\rangle = \underline{S}\vert\vec{F}_{\underline{a}})[\vec{G}^{c(2)}_{a,0}\vec{t}_{\underline{a}}(\vec{F}_{\underline{a}}\vert P\vert\Phi\rangle+\vec{G}^{c(2)}_{a}(\vec{F}_{\underline{a}}\vert\Delta u^c\vert\Phi\rangle]. \tag{23}$$

This is the integral representation of the generalized Faddeev equation (5).

## III. FORMULATION

To solve Eq. (23), we divide $G^{c(2)}_{\underline{a},0}t_{\underline{a}}$ as a separable term and the remainder. For this purpose, we introduce the first Sturm-Liouville function for the potential $\vec{V}_a+\vec{u}^c_a$. Among the infinite number of solutions of the homogeneous equation

$$\vec{G}^{c(2)}_{a,}\vec{V}_a\vert\vec{\psi}^c_{\underline{a}}\rangle = \lambda_{\underline{\bar{a}}}\vert\vec{\psi}^{\,c}_{\underline{a}}\rangle, \tag{24}$$

the first Sturm-Liouville function is the solution with the largest eigenvalue $\lambda_{\underline{\bar{a}}}$, which is determined by Eq. (24) for each $q$ and $\underline{\bar{a}}$. The function $\vec{\psi}^c_{\underline{\bar{a}}}$ is a function of $q$ and $x$. We normalize this function as

$$\langle\vec{\psi}^c_{\underline{\bar{a}}}\vert\vec{V}_a\vert\vec{\psi}^c_{\underline{a}}\rangle = -1. \tag{25}$$

The eigenvalue for the Reid soft core potential are shown in Fig. 1. The maximum eigenvalue for the coupled $^3S_1+^3D_1$ states is unity at $q=0.23140$ fm$^{-1}$, corresponding to the deuteron bound state. The values of $q$ necessary to the calculation of $^3$He are $q\gtrsim 0.38$ fm$^{-1}$. In this case, $1>\lambda_{\underline{\bar{a}}}>0$. Therefore, the iterative calculation of the two-body kernel

$$\vec{G}^{c(2)}_{\underline{a},0}\vec{t}_{\underline{a}} = \vec{G}^{c(2)}_{\underline{a},0}\vec{V}_a+\vec{G}^{c(2)}_{\underline{a},0}\vec{V}_a\vec{G}^{c(2)}_{\underline{a},0}\vec{V}_a+\cdots \tag{26}$$

converges. However, the convergence is very slow around those values of $q$ not very much larger than $q=0.38$. To overcome this inconvenience, we express this kernel up to a certain value $q_M$ as[22]

$$\vec{G}^{c(2)}_{a,0}\vec{t}_{\underline{a}} = -\vert\vec{\psi}^c_{\underline{a}}\rangle\langle\vec{\psi}^c_{\underline{a}}\vert\vec{V}_a+(\vec{\omega}^c_{\underline{a}}-1) \quad (q_M\geqq q) \tag{27}$$

for $^1S_0$ and $^3S_1+^3D_1$ states. Here

$$\vec{\psi}^c_{\underline{a}} = [\lambda_{\underline{\bar{a}}}/(1-\lambda_{\underline{\bar{a}}})]^{1/2}\vec{\psi}^c_{\underline{a}}, \tag{28}$$

and

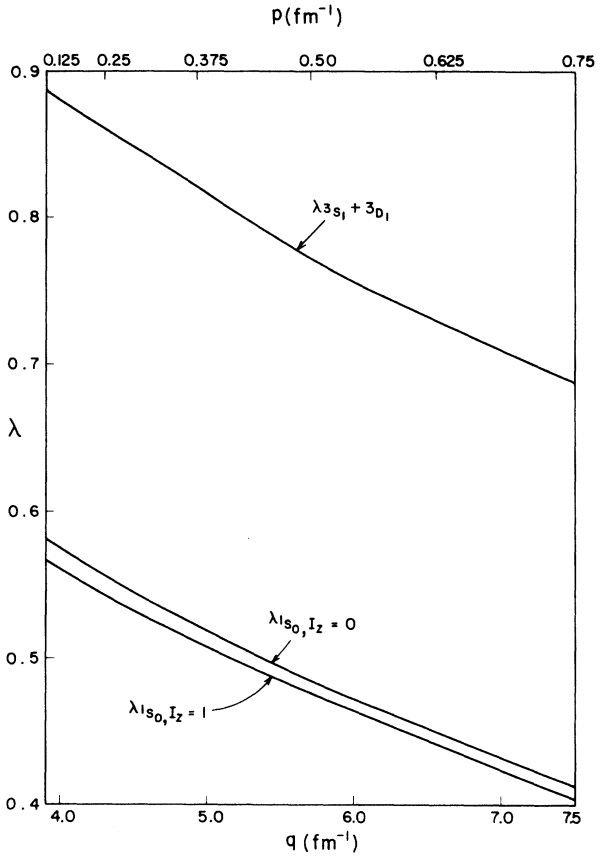


FIG. 1. The first eigenvalue λ of the Sturm-Liouville functions for the Reid soft core potential. In the $^1S_0$, $I_z=1$ state, the Coulomb potential is also involved.

$$\vec{\omega}^c_{\underline{a}} = \vec{1} + \vec{g}^c_{\underline{a}} \vec{V}_a \vec{\omega}^c_{\underline{a}}, \tag{29}$$

where the Green's function $\vec{g}^c_{\underline{a}}$ is defined by

$$\vec{g}^c_{\underline{a}} = \vec{G}^{c(2)}_{\underline{a},0} + \lambda_{\underline{a}} |\vec{\psi}^c_{\underline{a}}\rangle\langle\vec{\psi}^c_{\underline{a}}| . \tag{30}$$

A large part of $\vec{G}^{c(2)}_{\underline{a},0}\vec{V}_a$, which makes the series (26) very slowly convergent has been absorbed in the denominator $(1-\lambda_{\underline{a}})^{-1}$ of Eq. (28). Since the new kernel $\vec{g}^c_{\underline{a}}\vec{V}_a$ is orthogonal to the kernel $|\vec{\psi}^c_{\underline{a}}\rangle\langle\vec{\psi}^c_{\underline{a}}|\vec{V}_a$, it is small. As a result, the term $(\vec{\omega}^c_{\underline{a}} - \vec{1})$ in Eq. (27) is small and may be treated as a perturbation when we put Eq. (27) into Eq. (23).

We call those states $\vec{\underline{a}}$, for which we use Eq. (27), "the basic states." More precisely, the basic states consist of the states with the quantum numbers $^1S_0$ or $^3S_1+^3D_1$ and momentum $q \leqq q_M$. We call all other states nonbasic. For nonbasic states, the kernel $\vec{G}^{c(2)}_{\underline{a},o}\vec{t}_{\underline{a}}$ is small, and, in calculations of Eq. (23), we treat this kernel as a perturbation without decomposing as Eq. (27). The last term in Eq. (23) is also treated as the perturbation.

According to the above prescription, we divide the sum $S$ in Eq. (23) into the sum over basic states $S^B$ and over nonbasic states $S^{NB}$,

$$\begin{aligned}|\Phi\rangle = &\sum_{\vec{\alpha}}^{S^B} |\vec{F}_{\underline{\alpha}}\rangle[-|\vec{\psi}^c_{\underline{a}}\rangle\langle\vec{\psi}^c_{\underline{a}}|\vec{V}_a + (\vec{\omega}^c_{\underline{a}} - \vec{1})](\vec{F}_{\underline{\alpha}}|P|\Phi\rangle \\ &+ \sum_{\vec{\alpha}}^{S^{NB}} |\vec{F}_{\underline{\alpha}}\rangle\vec{G}^{c(2)}_{\underline{a},o}\vec{t}_{\underline{a}}(\vec{F}_{\underline{\alpha}}|P|\Phi\rangle \\ &+ \sum_{\vec{\alpha}}^{S} |\vec{F}_{\underline{\alpha}}\rangle\vec{G}^{c(2)}_{\underline{a}}(\vec{F}_{\underline{\alpha}}|\Delta u^c|\Phi\rangle . \end{aligned} \tag{31}$$

To express the right hand side of Eq. (31) compactly, we put

$$\gamma_{\vec{\alpha}} = \langle\vec{\psi}^c_{\underline{a}}|\vec{V}_a(\vec{F}_{\underline{\alpha}}|P|\Phi\rangle \tag{32}$$

and

$$\begin{aligned} C = &\sum_{\vec{\alpha}}^{S^B} |\vec{F}_{\underline{\alpha}}\rangle(\vec{\omega}^c_{\underline{a}} - \vec{1})(\vec{F}_{\underline{\alpha}}|P + \sum_{\vec{\alpha}}^{S^{NB}} |\vec{F}_{\underline{\alpha}}\rangle\vec{G}^{c(2)}_{\underline{a},o}\vec{t}_{\underline{a}}(\vec{F}_{\underline{\alpha}}|P \\ &+ \sum_{\vec{\alpha}}^{S} |\vec{F}_{\underline{\alpha}}\rangle\vec{G}^{c(2)}_{\underline{a}}(\vec{F}_{\underline{\alpha}}|\Delta u^c . \end{aligned} \tag{33}$$

Then, Eq. (31) reads

$$|\Phi\rangle = -\sum_{\vec{\alpha}}^{S^B} |\vec{F}_{\underline{\alpha}}\cdot\vec{\psi}^c_{\underline{a}}\rangle\gamma_{\vec{\alpha}} + C|\Phi\rangle , \tag{34}$$

where for coupled states $\vec{F}_{\underline{\alpha}}\cdot\vec{\psi}^c_{\underline{a}}$ denotes $F(^3S_1)\psi^c \times (^3S_1) + F(^3D_1)\psi^c(^3D_1)$. Namely, it represents a function like a scalar product of two vectors $\vec{F}_{\underline{\alpha}}$ and $\vec{\psi}^c_{\underline{a}}$. For the same reason, $C$ is a $1\times 1$ matrix.

If we write

$$|\Phi^{\vec{\beta}}_{\underline{\beta}}\rangle = (1-C)^{-1}|\vec{F}_{\underline{\beta}}\cdot\vec{\psi}^c_{\underline{b}}\rangle , \tag{35}$$

Eq. (34) reads

$$|\Phi\rangle = -\sum_{\vec{\beta}}^{S^B} |\Phi^{\vec{\beta}}_{\underline{\beta}}\rangle\gamma_{\vec{\beta}} . \tag{36}$$

We put Eq. (36) into Eq. (32) to obtain a coupled set of algebraic equations for $\gamma_{\vec{\alpha}}$,

$$\gamma_{\vec{\alpha}} = -\sum_{\vec{\beta}}^{S^B} M_{\vec{\alpha},\vec{\beta}}\gamma_{\vec{\beta}} , \tag{37}$$

where

$$M_{\vec{\alpha},\vec{\beta}} = \langle\vec{\psi}^c_{\underline{a}}|\vec{V}_a(\vec{F}_{\underline{\alpha}}|P|\Phi^{\vec{\beta}}_{\underline{\beta}}\rangle . \tag{38}$$

The homogeneous equation (31), as well as Eq. (37), are satisfied at the bound state.

Now, we have to calculate the function $|\Phi^{\vec{\beta}}_{\underline{\beta}}\rangle$. For this purpose, we express $|\Phi^{\vec{\beta}}_{\underline{\beta}}\rangle$ as

$$|\Phi^{\vec{\beta}}_{\underline{\beta}}\rangle = \sum_{\vec{\alpha}}^{S} |\vec{F}_{\underline{\alpha}}\rangle|\vec{\phi}^{\vec{\beta}}_{\vec{\alpha}}\rangle , \tag{39}$$

and compare Eq. (39) with the equation obtained from Eq. (35),

$$|\Phi^{\vec{\beta}}_{\underline{\beta}}\rangle = |\vec{F}_{\underline{\beta}}\cdot\vec{\psi}^c_{\underline{b}}\rangle + C|\Phi^{\vec{\beta}}_{\underline{\beta}}\rangle . \tag{40}$$

Noting that $C$ is given by Eq. (33), we obtain the following results; if $\vec{\alpha}$ belongs to the basic states,

$$|\vec{\phi}^{\vec{\beta}}_{\vec{\alpha}}\rangle = \delta_{\vec{\alpha},\vec{\beta}}|\vec{\psi}^{c}_{\vec{b}}\rangle + (\vec{\omega}^{c}_{\vec{a}} - \vec{1})(\vec{F}_{\vec{\alpha}}|P|\Phi_{\vec{\beta}}\rangle + \vec{G}^{c(2)}_{\vec{a}}(\vec{F}_{\vec{\alpha}}|\Delta u^{c}|\Phi_{\vec{\beta}}\rangle, \quad (41a)$$

and if $\vec{\alpha}$ does not belong to the basic states,

$$|\vec{\phi}^{\vec{\beta}}_{\vec{\alpha}}\rangle = \vec{G}^{c(2)}_{a,o}\vec{t}_{\vec{a}}(\vec{F}_{\vec{\alpha}}|P|\Phi_{\vec{\beta}}\rangle + \vec{G}^{c(2)}_{\vec{a}}(\vec{F}_{\vec{\alpha}}|\Delta u^{c}|\Phi_{\vec{\beta}}\rangle. \quad (41b)$$

If we define a function $|\vec{\xi}^{\vec{\beta}}_{\vec{\alpha}}(x)\rangle$ by

$$|\vec{\xi}^{\vec{\beta}}_{\vec{\alpha}}\rangle = \vec{G}^{c(2)}_{\vec{a}}[\vec{V}_{a}(\vec{F}_{\vec{\alpha}}|P|\Phi_{\vec{\beta}}\rangle + (\vec{F}_{\vec{\alpha}}|\Delta u^{c}|\Phi_{\vec{\beta}}\rangle] \quad (42)$$

and make use of Eqs. (27) and (38), Eqs. (41a) and (41b) are expressed as

$$|\vec{\phi}^{\vec{\beta}}_{\vec{\alpha}}\rangle = |\vec{\psi}^{c}_{\vec{a}}\rangle(\delta_{\vec{\alpha},\vec{\beta}} + M_{\vec{\alpha},\vec{\beta}}) + |\vec{\xi}^{\vec{\beta}}_{\vec{\alpha}}\rangle,$$

for $\vec{\alpha}$ belonging to the basic states, (43)

and

$$|\vec{\phi}^{\vec{\beta}}_{\vec{\alpha}}\rangle = |\vec{\xi}^{\vec{\beta}}_{\vec{\alpha}}\rangle,$$

for $\vec{\alpha}$ not belonging to the basic states. (44)

If we put Eqs. (43) and (44) in Eq. (39), Eq. (36) becomes

$$|\Phi\rangle = -\underset{\vec{\beta}}{S^{B}}\{\underset{\vec{\alpha}}{S^{B}}|\vec{F}_{\vec{\alpha}}\rangle[|\vec{\psi}^{c}_{a}\rangle(\delta_{\vec{\alpha},\vec{\beta}} + M_{\vec{\alpha},\vec{\beta}}) + |\vec{\xi}^{\vec{\beta}}_{\vec{\alpha}}\rangle] + \underset{\vec{\alpha}}{S^{NB}}|\vec{F}_{\vec{\alpha}}\rangle|\vec{\xi}^{\vec{\beta}}_{\vec{\alpha}}\rangle\}\gamma_{\vec{\beta}}. \quad (45)$$

In the case that Eq. (37) is satisfied, Eq. (45) is reduced to

$$|\Phi\rangle = -\underset{\vec{\alpha}}{S}|\vec{F}_{\vec{\alpha}}\rangle\underset{\vec{\beta}}{S^{B}}|\vec{\xi}^{\vec{\beta}}_{\vec{\alpha}}\rangle\gamma_{\vec{\beta}}. \quad (46)$$

If we put Eq. (42) into Eq. (46) and use Eq. (36), we see that Eq. (46) satisfies the generalized Faddeev equation. On the other hand, if Eq. (37) is not satisfied, Eq. (36) is expressed by virtue of Eq. (39) as

$$|\Phi\rangle = -\underset{\vec{\alpha}}{S}|\vec{F}_{\vec{\alpha}}\rangle\underset{\vec{\beta}}{S^{B}}|\vec{\phi}^{\vec{\beta}}_{\vec{\alpha}}\rangle\gamma_{\vec{\beta}}. \quad (47)$$

This function does not satisfy the generalized Faddeev equation. Since, in the course of iterations, neither the generalized Faddeev equation nor Eq. (37) is satisfied, Eq. (47) should be used.

*The iterative procedure.* Let us explain how to handle the above equations to obtain the solution. We put

$$\vec{\phi}^{\vec{\beta}}_{\vec{\alpha}}(x) = \sum_{m=0}^{\infty}\vec{\phi}^{\vec{\beta}(m)}_{\vec{\alpha}}(x). \quad (48)$$

The first term on the right hand side of Eq. (43) is taken as the zeroth order function

$$\vec{\phi}^{\vec{\beta}(0)}_{\vec{\alpha}}(x) = \begin{cases} \vec{\psi}^{c}_{\vec{a}}(x)\delta_{\vec{\alpha},\vec{\beta}}, & \text{if } \vec{\alpha} \text{ belongs to the basic states} \\ 0, & \text{if } \vec{\alpha} \text{ does not belong to the basic states.} \end{cases} \quad (49)$$

For $m \geq 1$, Eq. (43) without the first term and Eq. (44) are used,

$$\vec{\phi}^{\vec{\beta}(m)}_{\vec{\alpha}}(x) = \begin{cases} \vec{\psi}^{c}_{a}(x)M^{(m-1)}_{\vec{\alpha},\vec{\beta}} + \vec{\xi}^{\vec{\beta}(m)}_{\vec{\alpha}}(x), & \text{if } \vec{\alpha} \text{ belongs to the basic states,} \\ \vec{\xi}^{\vec{\beta}(m)}_{\vec{\alpha}}(x), & \text{if } \vec{\alpha} \text{ does not belong to the basic states.} \end{cases} \quad (50)$$

Corresponding to Eq. (38), $M^{(m)}_{\vec{\alpha},\vec{\beta}}$ in Eq. (50) is defined by

$$M^{(m)}_{\vec{\alpha},\vec{\beta}} = \langle\vec{\psi}^{c}_{\vec{a}}|\vec{V}_{a}|\chi^{\vec{\beta}(m)}_{\vec{\alpha}}\rangle, \quad (51)$$

with

$$\vec{\chi}^{\vec{\beta}(0)}_{\vec{\alpha}}(x) = (\vec{F}_{\vec{\alpha}}|P|\vec{F}_{\vec{\beta}})\vec{\psi}^{c}_{\vec{b}}, \quad (52)$$

and for $m \geq 1$

$$\vec{\chi}^{\vec{\beta}(m)}_{\vec{\alpha}}(x) = \underset{\vec{\alpha}'}{S}(\vec{F}_{\vec{\alpha}}|P|\vec{F}_{\vec{\alpha}'})\vec{\phi}^{\vec{\beta}(m)}_{\vec{\alpha}'}. \quad (53)$$

For all $\vec{\alpha}$, the function $\vec{\xi}^{\vec{\beta}(m)}_{\vec{\alpha}}$ in Eq. (50) is calculated by the following equation obtained from Eqs. (42), (39), and (53),

$$\vec{\xi}^{\vec{\beta}(m)}_{\vec{\alpha}}(x) = \vec{G}^{c(2)}_{\vec{a}}[\vec{V}_{a}\vec{\chi}^{\vec{\beta}(m-1)}_{\vec{\alpha}} + \vec{\eta}^{\vec{\beta}(m-1)}_{\vec{\alpha}}], \quad (54)$$

where $\vec{\eta}^{\vec{\beta}(m)}_{\vec{\alpha}}(x)$ is defined by

$$\vec{\eta}^{\vec{\beta}(m)}_{\vec{\alpha}}(x) = \underset{\vec{\alpha}'}{S}(\vec{F}_{\vec{\alpha}}|\Delta u^{c}|\vec{F}_{\vec{\alpha}'})\vec{\phi}^{\vec{\beta}(m)}_{\vec{\alpha}'}. \quad (55)$$

If the iteration converges, the function $\vec{\phi}^{\vec{\beta}}_{\vec{\alpha}}(x)$ given by Eq. (48) satisfies Eqs. (43) and (44). When Eq. (37) is satisfied for

$$M_{\vec{\alpha},\vec{\beta}} = \sum_{m=0}^{\infty}M^{(m)}_{\vec{\alpha},\vec{\beta}}, \quad (56)$$

Eq. (46) is obtained. As a result, the sum (48) is the solution of the generalized Faddeev equation.

In practice, we solve Eq. (54) as an ordinary

differential equation. The most difficult parts are the numerical calculations of the terms involving the particle exchange operator $P$, namely, Eqs. (52), (53), and (55). For $^3$H, where the spectator is free from any interaction, we may manipulate the transformation from one set of coordinates to another by Eq. (29) of Ref. 4. However, for $^3$He, if the spectator is a proton and under the influence of the modified Coulomb interaction, there is no analytical method for the transformation and we must rely on a numerical method. For the case of the $s$-wave spectator, to which we restrict ourselves, we can readily derive the following expression,

$$\left.\begin{matrix}\chi^{\vec{\beta}(m)}_{\vec{\alpha}}(x)\\ \eta^{\vec{\beta}(m)}_{\vec{\alpha}}(x)\end{matrix}\right\} = \sum_{\alpha'} N_{\alpha\alpha'} \int_0^\infty dp' \int_0^\infty y^2 dy\, F_\alpha(p,y)\frac{2}{xy}\int_{x'_{\min}}^{x'_{\max}} x'dx' P_L(\cos\theta_{\hat{x}\hat{x}'}) \left\{\begin{matrix}1\\ [v^c(x)-\bar{v}^c(y')]\end{matrix}\right\} F_{\alpha'}(p',y')\phi^{\vec{\beta}(m)}_{\vec{\alpha}'}(q',x') . \tag{57}$$

Here $N_{\alpha\alpha'}$ denotes the transformation coefficient of spin and isospin,

$$N_{\alpha\alpha'} \equiv \langle I I_z;\ \tfrac{1}{2}\, m_t; M_T(12,3) | I' I'_z;\ \tfrac{1}{2}\, m'_t; M_T(23,1)\rangle \times \langle (S\tfrac{1}{2}) S_0 M_{S_0}(12,3) | (S'\tfrac{1}{2}) S_0 M_{S_0}(23,1)\rangle . \tag{58}$$

The value of $N_{\alpha\alpha'}$ is given by Table II. The function $\eta^{\vec{\beta}(m)}_{\vec{\alpha}}(x)$ is nonzero only for $\alpha$ = No. 2, i.e., for the $^1S_0$ state with $I_z = 1$ for $^3$He. The relation between the set of coordinates $(x,y)$ and $(x',y')$ is given by

$$\vec{x}' = -\frac{\vec{x}}{2} - \vec{y}, \quad \vec{y}' = \frac{3}{4}\vec{x} - \frac{1}{2}\vec{y} \tag{59}$$

and

$$x'_{\min} = \left|\frac{x}{2} - y\right| , \quad x'_{\max} = \frac{x}{2} + y .$$

In concluding this section, we remark that if we use the values in Table II to the Faddeev equation, the equality

$$\phi_{^1S_0, I_z=0} = \frac{1}{\sqrt{2}}\phi_{^1S_0, I_z=1} \tag{60}$$

holds if there is no Coulomb interaction in the three-body system.

## IV. NUMERICAL CALCULATIONS AND RESULTS

### A. Numerical procedure

In numerical calculations, we take the maximum value of $p$ as 1.9504 fm$^{-1}$. In Fig. 11 of Ref. 4, it is seen that this value is sufficient. By Eq. (3), $q$ is related to $p$ and $|E|$. The value of $p_M$ that corresponds to $q_M$ of Eq. (27) is set to 0.75043 fm$^{-1}$. We divide the interval (0, 0.75043) into six equal intervals. To each mesh point of $p$ corresponds one value of $q$, for which we calculate the Sturm-Liouville function. The number of discretized basic states is thus $3\times 6$. Here, 3 is the number of states; two $^1S_0$ states with $I_z = 0$ and 1 and one coupled $^3S_1 + {}^3D_1$ state. As a result, the matrix $M_{\vec{\alpha},\vec{\beta}}$ defined by Eq. (38) in an $18\times 18$ matrix. Beyond $p = 0.75043$ fm$^{-1}$, we discretize continuous values of $p$ into six intervals of size 0.2 fm$^{-1}$. This part is treated as the perturbation, which is involved in the sum $S^{NB}$ of Eq. (31). We take $\Lambda$ of Eq. (10) as 2 fm$^{-1}$.

TABLE II. Transformation coefficient of spin and isospin $N_{\alpha\alpha'}$ defined by Eq. (58).

| State | | No. 1 | No. 2 | No. 3 | |
|---|---|---|---|---|---|
| State components | | 1 ($^1S_0, I_z=0$) | 2 ($^1S_0, I_z=1$) | 3 ($^3S_1, I_z=0$) | 4 ($^3D_1, I_z=0$) |
| No. 1 | 1 | $-\frac{1}{4}$ | $\frac{1}{2\sqrt{2}}$ | $-\frac{\sqrt{3}}{4}$ | 0 |
| No. 2 | 2 | $\frac{1}{2\sqrt{2}}$ | 0 | $-\frac{\sqrt{3}}{2\sqrt{2}}$ | 0 |
| No. 3 | 3 | $-\frac{\sqrt{3}}{4}$ | $-\frac{\sqrt{3}}{2\sqrt{2}}$ | $\frac{1}{4}$ | 0 |
| | 4 | 0 | 0 | 0 | $-\frac{1}{2}$ |

In order to speed up the calculation, keeping enough accuracy near the origin of the relative coordinate of the interacting pair, we set up an uneven $x$ mesh by the following formula

$$t(x) = C(x+T)x/(x+S), \tag{61}$$

with equidistant $t$ mesh. The parameter $C$ determines the slope $(dt/dx)_{x\to\infty}$ while the parameters $T$ and $S$ are chosen so that (i) at $t=t_0$, $x=x_0$, and (ii) at $x=0$, $dt/dx=\mu$, for preassigned values of $t_0$, $x_0$, and $\mu$. We use 0.3 fm for the $t$-mesh size, $t_0=9$ fm, $x_0=6$ fm, and $\mu=12$. The inverse transformation $x(t)$ is easily found. The first $x$ mesh point is $x_1=0.0259205$ fm, while $x_{30}-x_{29}=0.68626$ fm. Equation (54) is solved numerically as the inhomogeneous differential equation by the Numerov algorithm from the origin to $x_M=x_{38}=12.6339$ fm. Beyond this point $x_M$, the inhomogeneous term is sufficiently small due to the short range character of $\vec{\eta}^{\vec{\delta}(m)}_{\vec{\alpha}}(x)$ of Eq. (55) as well as $V_\alpha$.

In Eq. (57), at every mesh point of $x \leqq x_M$, the integral over $y$ is performed until $x'_{\min}$ becomes larger than 20 fm. For the $y$ mesh, we use a transformation $t(y)$ similar to Eq. (61), but with $C=0.3$, $t_0=18$ fm, $y_0=30$ fm, $t$-mesh size $=0.36$ fm, and $\mu=2$. This yields $y_1=0.184369$ fm, while $y_{50}-y_{49}=1.0156$ fm.

To perform numerical quadratures involving oscillatory functions $F_\alpha(p,y)$ and $F_{\alpha'}(p',y')$ in Eq. (57) accurately, we use a double spline interpolation on smooth varying parts of the integrand to speed up the calculation. Except for the zeroth order calculation, the integral over $p'$ is carried out first to ensure smooth $x'$ and $y'$ dependences. The $x'$ integration from $x'_{\min}$ to $x'_{\max}$ is done by the Simpson method with a small enough step size.

In calculating the solution vector $\gamma_{\vec{\alpha}}$ of the homogeneous algebraic equation (37), we use the same method as explained in Ref. 4. The residual $D$ as defined in Ref. 4 is very sensitive to energy, and we can determine the binding energy accurately.

For safety, we also calculated $^3$H using the same computer code PERFECT III as for $^3$He but with the Coulomb interaction turned off, and compared the result obtained from the code PERFECT I,[18] made for calculating $^3$H. We obtained remarkable agreement.

### B. Binding energy, Coulomb energy difference

In Table III, the calculated results are summarized together with the results obtained by other authors. As described in Sec. I, all calculated binding energies of $^3$H with RSC3 agree, despite the difference in approaches. In Refs, 10 and 11, the binding energy of $^3$He was obtained by solving a set of partial differential equations expressed by the hyperspherical coordinates. This results in a small Coulomb energy difference $\Delta E_c$. Reference 11 yields 546 keV for RSC3 and 559 keV for RSC5. Although Ref. 10 does not write the result of nonperturbative calculation of $\Delta E_c$ for the pure Coulomb and RSC potentials, this calculation should yield a similar result. All the perturbational calculations[11,13,14] yield 0.61–0.63 MeV for $\Delta E_c$. Thus we have obtained a larger value for $\Delta E_c$ than in Ref. 11 and our value almost agrees with (or is 0.01 MeV larger than) the values calculated by the first order perturbation $\Delta E_c^{(1)}$ with RSC3.

### C. Charge form factor and mean square radius

The charge form factor of $^3$He that has so far appeared in all articles has been calculated using the wave function of $^3$H, except so far by Gignoux and Laverne,[10] where the Coulomb and a charge asym-

TABLE III. Summary of $^3$H and $^3$He properties for the Reid soft core potential. The dagger denotes the value for $s$-wave projected Coulomb potential. $\Delta E_c^{(1)}$ is the value from the first order perturbation calculation. RSCN ($N=3,4,5$) indicates partial waves which are taken into account (see Introduction of the text). CA denotes the inclusion of a charge asymmetric potential (Ref. 23). $P(S')$, $P(D)$, and $P(T=\frac{3}{2})$ are probabilities in % of the $S'$, $D$, and $T=\frac{3}{2}$ states.

| | $^3$H | $^3$He | $\Delta E_c$ | $\Delta E_c^{(1)}$ | $^3$H $P(S')$ | $^3$H $P(D)$ | $^3$He $P(S')$ | $^3$He $P(D)$ | $P(T=\frac{3}{2})$ | |
|---|---|---|---|---|---|---|---|---|---|---|
| Expt. | 8.482 | 7.718 | 0.764 | | | | | | | |
| Ours | 6.400 | 5.775 | 0.625 | | 1.91 | 8.02 | 2.265 | 7.970 | $2.16\times10^{-3}$ | RSC3 |
| PGF[a] | 6.38 | 5.83 | 0.546† | 0.614 | 1.88 | 8.01 | 1.88/2.21 | 8.01/8.06 | | RSC3 |
| | 7.01 | 6.45 | 0.558† | 0.616 | 1.68 | 9.11 | 1.66/1.93 | 9.10/9.17 | | RSC5 |
| GL[b] | 6.44 | 5.80 | 0.64 | 0.61 | 2.0 | 7.8 | 2.6 | 7.9 | $2\times10^{-3}$ | CA |
| MT[c] | 6.9 | 6.27 | | 0.63 | 1.6 | 8.5 | | | | RSC4 |

[a]Reference 11.
[b]Reference 10.
[c]Reference 14.

metric force[23] were taken into account. Therefore Fig. 2, that shows the charge form factor of $^3$He calculated with and without Coulomb interaction, is the first presentation of the pure Coulomb effect to the charge form factor. The wave function involving the Coulomb effect shifts the minimum at $q^2 = 15.2$ fm$^{-2}$ (without Coulomb) only a little ($q^2 \simeq 0.5$ fm$^{-2}$) toward small momentum transfer. This is, of course, a result of the enlargement of the system due to the Coulomb repulsion. The root mean square radius of $^3$He is 2.033 fm (1.999 fm) with (without) the Coulomb interaction, whereas the experimental value is $1.84 \pm 0.03$ fm.[24]

### D. Properties of Faddeev components

In Ref. 4, we observed the following properties of a Faddeev component of the triton wave function: For a given value of the spectator momentum $p$, each Faddeev component had a node in its $^1S_0$ and $^3S_1$ states, but no node existed in the $^3D_1$ component (see Fig. 10 of Ref. 4). The node for the $S$ state is a direct consequence of the Faddeev decomposition of the total wave function. On the right hand side of Eq. (16), the overlap of $V(x_3)$ with the function $\Phi(23,1)$ [or $\Phi(31,2)$] causes this node because $\Phi(23,1)$ [$\Phi(31,2)$] describes the state in which the particle 1(2) can move freely to any place while the pair 23 (31) are interacting. As a consequence, $\Phi(23,1)$ and $\Phi(31,2)$ are proportional to $x_3^L$ as $x_3 \to 0$, and are multiplied by the interaction with a strong repulsive core to form the right hand side of Eq. (16). This causes the node seen in $^1S_0$ and $^3S_1$ states. For the $D$ state, however, the node does not appear because of the centrifugal barrier. This behavior for a Faddeev component of $^3$H manifests itself also in $^3$He as seen in Figs. 3–6. The function $\phi_{\vec{\alpha}}(p,x)$ in these figures is defined by

$$\phi_{\vec{\alpha}}(p,x) \equiv x \sum_{\vec{\beta}} S^B_{\vec{\beta}} \, | \, \xi^{\vec{\beta}}_{\vec{\alpha}} \rangle \gamma_{\vec{\beta}} \, . \tag{62}$$

The relation of this function to the function $\Phi(12,3)$ is given by Eq. (46). To normalize, we have to multiply by the normalization factor $N = 0.135\,33$ for $^3$He and $0.163\,14$ for $^3$H.

In Fig. 7, the behavior of the Faddeev components at large distances of $x_3$ is illustrated. We see that the sum of components $\Phi(23,1)$ and $\Phi(31,2)$ is still larger than the component $\Phi(12,3)$ at $x_3 = 12$ fm. In Fig. 7, the components are not normalized, but are shown with relative magnitude.

### E. Sum of Faddeev components

As given by Eq. (4), the wave function of $^3$H or $^3$He is the sum of the Faddeev components for different sets of coordinates. To add the contributions from other components $\Phi(23,1)$ and $\Phi(31,2)$, we express these functions in terms of the spec-

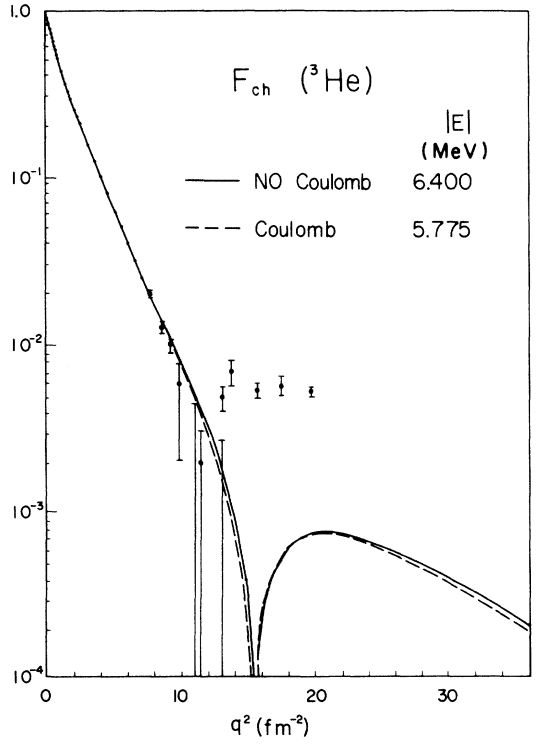


FIG. 2. Charge form factor of $^3$He with and without Coulomb interactions. Experimental values are taken from Ref. 24.

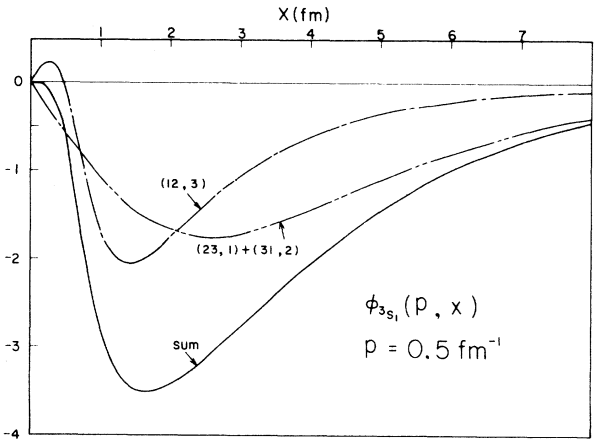


FIG. 3. The curve marked (12,3) represents the function $\phi_\alpha(p,x)$ for the $^3S_1$ state of $^3$He. This function is defined by Eq. (62). The curve marked (23,1) + (31,2) represents the function $\Xi_\alpha(p,x)$ defined by Eq. (63). Note a node of $\phi_\alpha(p,x)$ near the origin. This node disappears in the sum $\phi_\alpha(p,x) + \Xi_\alpha(p,x)$. The function $\Xi_\alpha(p,x)$ is rather long ranged owing to the exchange effect.

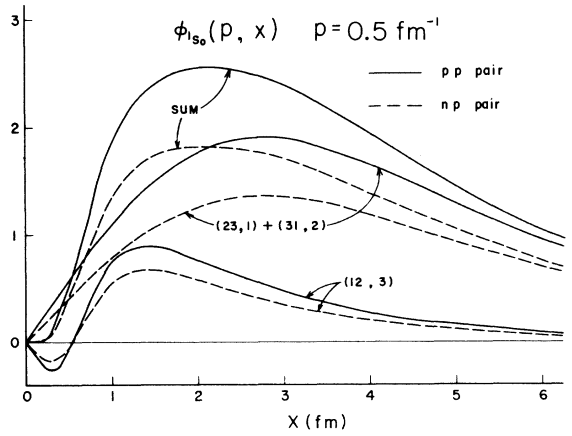


FIG. 4. The functions $\phi_\alpha(p,x)$ and $\Xi_\alpha(p,x)$ for the $^1S_0$ states of $^3$He (see caption of Fig. 3).

tator momentum $p$ of the particle 3 and the relative coordinate $x$ of the pair 12. We define a function $\Xi_{\vec{\alpha}}(p,x)$ by

$$\Phi(23,1)+\Phi(31,2)=-S\sum_{\vec{\alpha}}\tilde{F}_{\vec{\alpha}}(12,3)\Xi_{\vec{\alpha}}(p,x), \quad (63)$$

and

$$\Xi_{\vec{\alpha}}(p,x)=x\tilde{\Xi}_{\vec{\alpha}}(p,x). \quad (64)$$

In the sum $\phi_{\vec{\alpha}}(p,x)+\Xi_{\vec{\alpha}}(p,x)$, the node seen in the previous section disappears as shown in Figs. 3 and 4, while a node that moves into the origin with increasing spectator momentum appears in the $^3D_1$ state. This is illustrated in Figs. 5 and 6. This behavior also appears in the Fourier transform of the Brandenburg-Kim-Tubis wave function.[8,25]

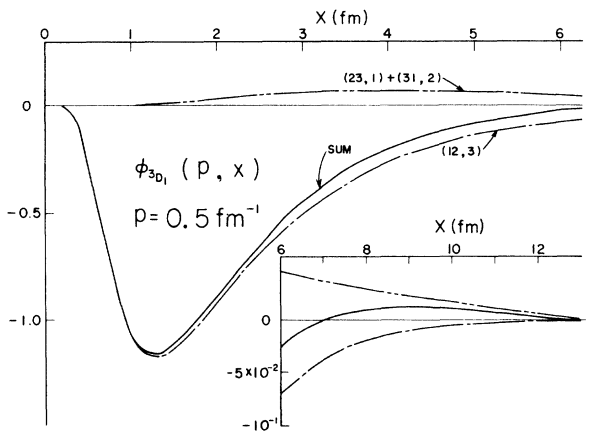


FIG. 5. The functions $\phi_\alpha(p,x)$ and $\Xi_\alpha(p,x)$ for the $^3D_1$ state of $^3$He. Each function has no node. But the sum of these functions has a node. A qualitative account is given in Sec. V B.

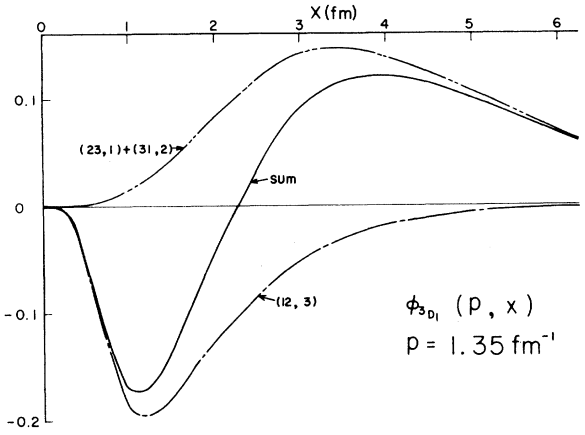


FIG. 6. The functions $\phi_\alpha(p,x)$ and $\Xi_\alpha(p,x)$ for the $^3D_1$ state of $^3$He (see caption of Fig. 5). We see that the node moves into the direction of small $x$, with increasing spectator momentum $p$. A qualitative discussion of this behavior is given in Sec. V B.

### F. Two-body correlations

The two-body correlation in $^3$H for RSC was studied in Ref. 7. This quantity affects various phenomena.[26] In the present paper, we compare the correlation functions for $^3$He and $^3$H.

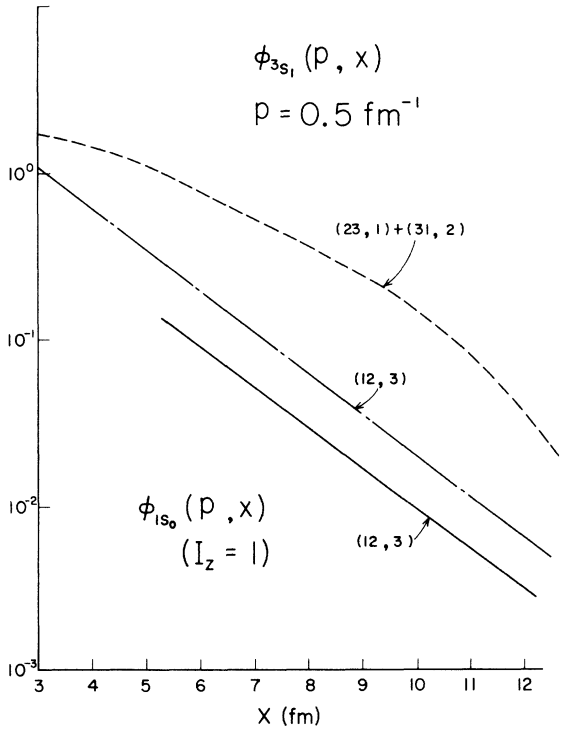


FIG. 7. The behaviors of $\phi_\alpha(p,x)$ and $\Xi_\alpha(p,x)$ at large distances $x$. Note that the function $\Xi_\alpha(p,x)$ does not show the asymptotic behavior at $x=12$ fm as yet.

We define the two-body correlation function for a state $\vec{\alpha}$ by

$$\rho_{\vec{\alpha}}(x) = \int_0^\infty |\phi_{\vec{\alpha}}(p,x) + \Xi_{\vec{\alpha}}(p,x)|^2 dp \,. \tag{65}$$

Figure 8 shows the correlation functions of the $^3S_1$ and the $^3D_1$ states in $^3$H. These are compared with the probability density of the $^3S_1$ and the $^3D_1$ states of the RSC deuteron. The correlation function and the probability density of each state are normalized to unity. From Fig. 8, we see that the correlation function has no node in the $^3D_1$ state, although the function $\phi_{\vec{\alpha}}(p,x) + \Xi_{\vec{\alpha}}(p,x)$ for this state has a node as we have seen in Figs. 5 and 6. The square root of the correlation function for $^3$H may be compared with the function $\bar{\phi}_3(r)$ illustrated in Fig. 3 of an article by Hajduk *et al.*[27] We see almost similar behaviors for both functions.

To see the Coulomb effect, Fig. 9 illustrates the correlation functions for the $^1S_0$, $^3S_1$, and $^3D_1$ states in $^3$He and $^3$H. The correlation function of each state is normalized to unity. Figure 10 shows the correlation functions of $^3$H and $^3$He summed up for all states. The sum is normalized to unity for each of $^3$He and $^3$H. The correlation functions for $^3$He and $^3$H differ by about $10^{-3}$ near 9 fm.

In concluding this subsection, we see that the behavior of our correlation functions for $^3$H is almost similar to that in Ref. 7. In $^3$He, the Coulomb potential pushes the correlation functions slightly outward. Before the normalization, there is no Coulomb effect at short distances. However, when the wave function is normalized to unity, the

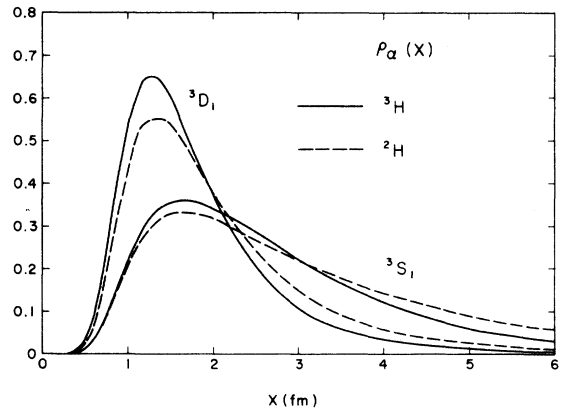


FIG. 8. The two-body correlation function defined by Eq. (65) for the $^3S_1$ and $^3D_1$ states in $^3$H. These functions are compared with the probability density of the $^3S_1$ and $^3D_1$ states of deuteron for RSC. The correlation function and probability density of each state are normalized to unity.

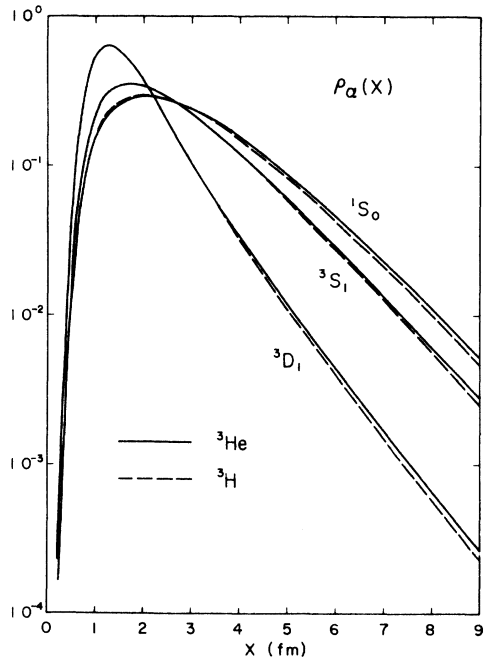


FIG. 9. The correlation functions for the $^1S_0$, $^3S_1$, and $^3D_1$ states in $^3$He and $^3$H. The correlation function of each state is normalized to unity.

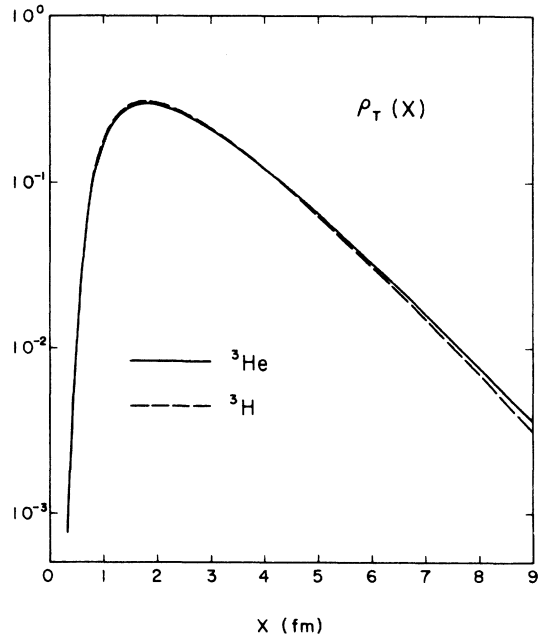


FIG. 10. The correlation functions of $^3$H and $^3$He summed up for all states. The sum is normalized to unity for each of $^3$He and $^3$H. We see a small Coulomb effect at large distances.

correlation function for $^3$He becomes smaller than that for $^3$H at short distances.

## V. DISCUSSIONS AND CONCLUSIONS

### A. Boundary conditions

We have used the function defined by Eq. (13) for the spectator. On the other hand, we have used the solution of Eq. (54) as the wave function of the interacting pair. These functions are regular at the origin of the coordinates $y$ and $x$, respectively.

At a large distance, if the spectator is charged, its wave function behaves as the Coulomb wave function with the phase shift resulting from a short range potential $-e^{-\Lambda y}\times e^2/y$ in Eq. (10). In the asymptotic region, the wave function is known in an analytic form. Also we can calculate it numerically with a sufficient accuracy. If the spectator is not charged, it is simply a spherical Bessel function.

For the interacting pair, the right hand side of Eq. (54) becomes negligibly small beyond, say, 12 fm. Then the wave function behaves as the irregular solution of the equation

$$(-\hbar^2q^2/M-\vec{T}_L-\vec{u}_a^c)\xi_{\underline{\alpha}}^{\vec{\beta}(m)}=0\,, \tag{66}$$

for which the analytic form is known, and again we can calculate it numerically with a sufficient accuracy. The function $\xi_{\underline{\alpha}}^{\vec{\beta}(m)}$ behaves asymptotically as

$$\xi_{\underline{\alpha}}^{\vec{\beta}(m)}\sim\frac{e^{-qx}}{x}(2qx)^{-Me^2/\hbar^2q}\,. \tag{67}$$

To summarize, we have imposed correct boundary conditions everywhere. On the other hand, the boundary condition $\partial F(\rho,\theta)/\partial\rho=0$ for $\rho=\rho_{\max}$ used in the hyperspherical approach[10,11] is yet to be justified when the system involves the Coulomb interaction.

### B. Properties of Faddeev components

Solving the three-body Schrödinger equation *à la mode de* Faddeev is now common, but the properties of the Faddeev components are not known very well, because most authors have solved the Faddeev equation in momentum space. In Secs. IV D and IV E, we have seen the following behavior of the Faddeev components for a fixed momentum $p$ of the spectator. The component $\phi_{\vec{\alpha}}(p,x)$ for the $^1S_0$ as well as the $^3S_1$ states of the interacting pair has a node near the origin, while the component for the $^3D_1$ state has no node of this kind. On the other hand, if we sum up three components to obtain $\phi_{\vec{\alpha}}(p,x)+\Xi_{\vec{\alpha}}(p,x)$, the node disappears for the $S$ states, while a node appears for the $D$ state at a large distance. This node disappears if we integrate over $p$ as seen in Sec. IV F. Although this behavior of the components is due to the Faddeev decomposition of the total wave function and by no means physical, it might be worthwhile to discuss the properties of the Faddeev components.

#### *1. Node near the origin*

As stated in Sec. IV D, the node near the origin appears as a consequence of the direct overlap of the potential $V(x_3)$ and the components $\Phi(23,1)$ or $\Phi(31,2)$. In the present paper, we are taking RSC as the potential, and there is no drastic consequence of this overlap, provided that we perform the calculations very carefully. However, if the potential $V(x_3)$ involves a hard core, this overlap becomes infinite. In this case, we should reformulate the theory with more suitable boundary conditions, so that no particle may enter into the core region. From this argument, we see that there must be a more physical formulation by which one can treat the potential with a soft core as well as with a hard core on the same basis. However, in such a formulation, the boundary condition becomes very complicated near the origin and we need more time and memory to solve the equation.

What we want to emphasize here is the following. Under the usual boundary condition, the Faddeev component for the $S$ state *should* have a node near the origin, if the potential has a soft core. To get this node in solving the Faddeev equation, we should calculate very carefully especially near the origin. For instance, if we want to calculate the Faddeev equation utilizing a set of harmonic oscillator wave functions, we need a prohibitively large number of quanta. Otherwise, the component $\phi_\alpha(p,x)$ for the $S$ state has no node, resulting in a larger (wrong) binding energy.[28]

#### *2. Node at a large distance*

In Sec. IV E, we have seen that the function $\phi_\alpha(p,x)+\Xi_\alpha(p,x)$ has no node for the $S$ states, while there is a node at a large distance for the $D$ state. In this subsection, we study these behaviors qualitatively.

First let us remark that except around the origin, the component $\phi_\alpha(p,x)$ for the $^1S_0$ state is positive both for $I_z=0$ and 1, while the components for the $^3S_1$ and $^3D_1$ states are negative (see, Figs. 3–6). The different signs of $^1S_0$ and $^3S_1$ components are due to our choice of the isospin function as given in Table I.

Next, we remark that from Figs. 3 and 4, we see an approximate relation

$$|\phi_{^3S_1}(p,x)| \simeq 3|\phi_{^1S_0,I_z=0}(p,x)| \quad (68)$$

holds.

Since the Coulomb effects are rather small compared with the nuclear effects, let us consider only the term $(F_{\underline{\alpha}}|VP|\phi\rangle$ in Eq. (16). If we neglect the Coulomb effect, the function $F_{l=0}(p,y)$ is approximated by

$$F_{l=0}(p,x) \simeq (2/\pi)^{1/2} p j_0(py). \quad (69)$$

The factors that affect the change of sign of a Faddeev component in going from one set of coordinates to another, for example, from (23,1) to (12,3) are the transformation coefficients $N_{\alpha\alpha'}$ and the overlap of angular functions. If we restrict ourselves to the basic states, we can readily derive the equation

$$(\vec{F}_{\underline{\alpha}}|P|\vec{F}_{\underline{\alpha}'})\phi_{\underline{\alpha}'}(x) = N_{\alpha\alpha'}\int_0^\infty x'^2 dx' \phi_{\underline{\alpha}'}(x') \times \int_{-1}^{1} d(\cos\theta_{\hat{x}\hat{x}'}) P_L(\cos\theta_{\hat{x}\hat{x}'}) \times F_{l=0}(p,y)F_{l=0}(p',y'). \quad (70)$$

The function $\Xi_{\vec{\alpha}}(p,x)$ is equal to twice of the sum of Eq. (70) over $\underline{\alpha}'$, namely, the sums over the states $\alpha'$ of Table II and the integration over $p'$.

Since $\phi_{\alpha'}(x')$ is a rather smooth function of $p'$, the integration over $p'$ of $p' j_0(p'y')\phi_{\alpha'}(x')$ is roughly proportional to $\delta(|\vec{x}'/2+\vec{x}|)$. This $\delta$ function is realized when the vectors $\vec{x}$ and $\vec{x}'$ are in the opposite direction with the magnitude $x=x'/2$. As a result,

$$\int_{-1}^{1} d(\cos\theta_{\hat{x}\hat{x}'}) P_L(\cos\theta_{\hat{x}\hat{x}'}) F_0(p,y)\int_0^\infty dp' F_0(p',y')\phi_{\underline{\alpha}'}(x') \simeq \frac{\delta(x-x'/2)}{xx'}\phi_{\alpha'}(q_0,x')\int_{-1}^{1} d(\cos\theta_{\hat{x}\hat{x}'}) \times \delta(\theta_{\hat{x}\hat{x}'}-\pi)F_0(p,y) \simeq \frac{\delta(x-x'/2)}{xx'}\phi_{\alpha'}(q_0,x')F_0(p,|\tfrac{1}{2}x-x'|), \quad (71)$$

where $q_0$ is some value at $q_M > q_0 > [(m/\hbar^2)|E|]^{1/2}$. Hence,

$$\sum_{\underline{\alpha}'}(F_{\underline{\alpha}}|P|F_{\alpha'})\phi_{\alpha'}(x) \simeq \sum_{\underline{\alpha}'} N_{\alpha\alpha'}\phi_{\alpha'}(q_0,2x)F_0(p,\tfrac{3}{2}x). \quad (72)$$

Since the function $F_0(p,\frac{3}{2}x)$ is positively definite so far as $px < \frac{2}{3}\pi$, the estimate (72) shows that the sign of $\Xi_\alpha(p,x)$ relative to $\phi_\alpha(p,x)$ depends only on $N_{\alpha\alpha'}$, which is given by Table II. For instance, $\Xi_\alpha(p,x)$ of the $^3D_1$ state is of the opposite sign from $\phi_\alpha(p,x)$, since $N_{\alpha\alpha'}=-\frac{1}{4}\delta_{\alpha\alpha'}$. As seen from (72), the functions $\Xi_\alpha(p,x)$ and $\phi_\alpha(p,x)$ depend very differently on $x_3$. As a result, this difference of the sign at a large distance causes a node in the $^3D_1$ state when $\Xi_\alpha(p,x)$ is added to $\phi_\alpha(p,x)$. Due to the function $F_0(p,\frac{3}{2}x)$ in Eq. (72), the node shifts to the direction of small $x$ with increasing $p$.

For the $S$ states, we see from Table II, the equality (60), and approximate relations (68) and (72), that the right hand side of (72) for $^1S_0$, $I_z=0$

$$\simeq\left(-\tfrac{1}{4}\phi_{^1S_0,I_z=0}+\frac{1}{2\sqrt{2}}\phi_{^1S_0,I_z=1}-\frac{\sqrt{3}}{4}\phi_{^3S_1}\right)F_0(p,\tfrac{3}{2}x) \simeq\left(-\frac{1}{4}+\frac{1}{2}+3\frac{\sqrt{3}}{4}\right)\phi_{^1S_0,I_z=0}(q_0,2x)F_0(p,\tfrac{3}{2}x). \quad (73)$$

As a result, the function $\Xi_\alpha(p,x)$ for the $^1S_0, I_z=0$ state is of the same sign as $\phi_\alpha(p,x)$ of this state. We can demonstrate this similarly for the $^1S_0$, $I_z=1$ and $^3S_1$ states, respectively.

### C. Summary and conclusions

Including the full Coulomb interaction for RSC3 and with correct boundary conditions, we have obtained the binding energy of $^3$He to be 5.775 MeV, which is 1.94 MeV less than the experimental value. We have obtained 6.400 MeV for the binding energy of $^3$H. This value agrees with Refs. 2–6. The Coulomb energy difference that we have obtained is 625 keV. This value is larger than the values obtained from the $s$ wave projected Coulomb interaction[11,12] and the first order perturbative calculations[10,11] with RSC3. However, our value is 15 keV less than the "expected" value of around 640 keV.[29]

We have seen, e.g., in Fig. 10, that the Coulomb effect enlarges the system. This results in a shift of the diffraction minimum of the charge form factor toward smaller momentum transfer as seen in Fig. 2. So far, the charge form factor of $^3$He has been calculated with the wave function of $^3$H. In the present paper, we have calculated this quantity with the wave function of $^3$He and compared with the result obtained from the wave function of $^3$H. We obtained the diffraction minimum of $^3$He at $q^2=15.2$ fm$^{-2}$ with the wave function of $^3$H and at 14.7 fm$^{-2}$ with the wave function of $^3$He. The root mean square radius of $^3$He is 1.999 fm for the wave function of $^3$H and 2.033 fm for the wave function of $^3$He.

We have found the complex behavior of a Faddeev component when it is expressed in terms of the spectator momentum $p$ and the relative distance of the interacting pair. The results were given in Sec. IV D. The qualitative discussions of these behaviors were given in Sec. V B.

In Fig. 7, we have seen that if the Faddeev

(23,1) and (31,2) components are expressed in terms of the set of coordinates $\vec{x}_3$ and $\vec{y}_3$, these components do not drop to the asymptotic value even at $x_3 = 12$ fm. This property does not harm the calculation of Eq. (5), since the interactions appearing on the right hand side of Eq. (5) are short ranged with respect to $x_3$. However, accurate calculations of quantities such as the isospin selection rule, magnetic form factor, etc., which are described by the direct overlap of wave functions without intervention by a potential, need a careful treatment of contributions from large distances.

In the present paper, we have focused our interest on a technique to calculate the Coulomb effect and a few direct consequences. Some quantities of physical interest, such as the dipole sum rule for $^3$He and the $(d,{}^3\text{He})$ asymptotic normalization constants, will appear elsewhere.

The subjects of the effect of $\Delta$, exchange currents, etc., will be treated in subsequent papers. Here let us remark that the present situation concerning the three-nucleon system can not be optimistic. It has been being clear that RSC is by no means "realistic" in the sense that this potential does not reproduce any three-nucleon properties correctly, and all other existing potentials are to be blamed for the same reason.[30] The three-nucleon force of the Fujita-Miyazawa type[31] was once thought to be encouraging, giving about 1 MeV of binding in triton.[32,33] However, it turned out in nuclear matter calculations that other three-nucleon contributions almost cancel the attraction of the three-nucleon force of the Fujita-Miyazawa type.[4,35] For the charge form factor, once the $\Delta$ contribution was thought to give a satisfactory magnitude,[36] but later it turned out that this was misleading and the $\Delta$ contribution is not so striking.[37] A consistent calculation of the nuclear potential and the exchange current has not been done as of yet, although Hadjimichael has obtained the overall good agreement with existing experimental data by using a three-body wave function derived from variational calculations with the admixture of the $\Delta$-resonance contribution.[38]

## ACKNOWLEDGMENTS

We gratefully acknowledge the Research Center for Nuclear Physics at Osaka University where the construction of PERFECT III was done with its computer. We would like to thank the Computer Center at the Research Institute for Plasma Physics, Nagoya University, for the generous support in the use of their computer for the production run. We express our gratitude to Professor T. Kawamura at the Institute for his hospitality. We express our hearty thanks to Mrs. N. Tichit at SPT, CEN-Saclay for her assistance in numerical calculations. This work was supported in part by the Japan Society for Promotion of Science.

[1] R. V. Reid, Ann. Phys. (N. Y.) 50, 411 (1968).
[2] R. A. Malfliet and J. A. Tjon, Ann. Phys. (N. Y.) 61, 425 (1970).
[3] E. P. Harper, Y. E. Kim, and A. Tubis, Phys. Rev. Lett. 28, 1533 (1972).
[4] T. Sasakawa and T. Sawada, Phys. Rev. C 19, 2035 (1979). Owing to an error in the phase of the $^3D_1$ state used in PERFECT I (see Ref. 18 below), the binding energy obtained in Ref. 4 is off by a certain amount. The correct value is given in the present paper.
[5] G. L. Payne, J. L. Friar, B. F. Gibson, and I. R. Afnan, Phys. Rev. C 22, 823 (1980).
[6] W. Glöckle (private communication).
[7] A. Laverne and C. Gignoux, Nucl. Phys. A203, 597 (1973).
[8] R. A. Brandenburg, Y. E. Kim, and A. Tubis, Phys. Rev. C 12, 1368 (1975).
[9] I. R. Afnan and N. D. Birrell, Phys. Rev. C 16, 823 (1977).
[10] C. Gignoux and A. Laverne, *Few Particle Problems in the Nuclear Interaction*, edited by I. Slaus *et al.* (North-Holland, Amsterdam, 1972), p. 411.
[11] G. L. Payne, B. F. Gilson, and J. L. Friar, Phys. Rev. C 22, 832 (1980).
[12] Laverne and Gignoux have obtained the Coulomb energy difference of 575 keV (Ref. 7). However, in what manner they obtained this value is not clearly written. No description about the wave function of $^3$He for RSC with the Coulomb interaction is found in Ref. 7.
[13] M. Haftel, Phys. Rev. C 14, 698 (1976).
[14] R. A. Malfliet and J. A. Tjon, *Few Particle Problems in the Nuclear Interaction*, edited by I. Slaus *et al.* (North-Holland, Amsterdam, 1972), p. 441.
[15] T. A. Osborn, J. Math. Phys. 14, 373 (1973); 14, 1485 (1973).
[16] L. D. Faddeev, *Mathematical Aspects of the Three-Body Problem in the Quantum Scattering Theory*, translated from Russian, the Israel Program for Scientific Translations (Davey, New York, 1965).
[17] T. Sasakawa and T. Sawada, Phys. Rev. C 20, 1954 (1979).
[18] T. Sasakawa and T. Sawada, Sci. Rep. Tohoku Univ. Ser. I: LXI, 70 (1978). The spherical harmonics $Y^{k*\kappa}_{L1}(\widehat{\lambda_1 p_1}, 0)$ in Eqs. (13) and (94) of this reference should read $Y^{k*\kappa}_{L1}(\widehat{\lambda_1 p_1}, \pi)$. Correspondingly, the right hand side of the seventh line from the bottom in p. 120 must be multiplied by *(-1.)**KL.
[19] T. Sasakawa, T. Sawada, and Y. E. Kim (unpublished).
[20] T. Sasakawa, T. Sawada, and Y. E. Kim, Phys. Rev. Lett. 45, 1386 (1980).
[21] T. Sasakawa and T. Sawada, Phys. Rev. C 22, 320 (1980).
[22] T. Sasakawa and T. Sawada, Prog. Theor. Phys. Suppl. 61, 1 (1977).

[23]E. M. Henly and T. E. Keliher, Nucl. Phys. A189, 632 (1972).
[24]J. S. McCarthy, I. Sick, and R. R. Whitney, Phys. Rev. C 15, 1396 (1977).
[25]Y. E. Kim (private communication).
[26]E. Hadjimichael, E. Harms, and V. Newton, Phys. Rev. Lett. 29, 1322 (1971); M. Chemtob and M. Rho, Nucl. Phys. A163, 1 (1971); E. Hadjimichael, S. N. Yang, and G. E. Brown, Phys. Lett. 39B, 594 (1972).
[27]Ch. Hajduk, A. M. Green, and M. E. Sainio, Nucl. Phys. A337, 13 (1980).
[28]W. Glöckle and R. Offermann, Phys. Rev. C 16, 2039 (1977).
[29]M. Fabre de la Ripelle, Fizika 4, 1 (1972); J. L. Friar, Nucl. Phys. A156, 43 (1970); J. L. Friar and B. F. Gibson, Phys. Rev. C 17, 1752 (1978).
[30]J. Chavin, C. Gignoux, J. J. Benayoun, and A. Laverne, Phys. Lett. 78B, 5 (1978).
[31]J. Fujita and H. Miyazawa, Prog. Theor. Phys. 17, 360 (1957).
[32]S. N. Yang, Phys. Rev. C 10, 2067 (1974).
[33]M. Sato, Y. Akaishi, and H. Tanaka, Prog. Theor. Phys. Suppl. 56, 76 (1974).
[34]T. Ueda, T. Sawada, and S. Takagi, Nucl. Phys. A285, 429 (1977).
[35]M. Martzolf, B. Loiseau, and P. Grange, Phys. Lett. 92B, 46 (1980).
[36]M. M. Giannini *et al.*, quoted in D. Drechsel, Nucl. Phys. A335, 17 (1980).
[37]J. A. Tjon and P. Sauer (private communication).
[38]E. Hadjimichael, Nucl. Phys. A294, 513 (1978).